Lateral Torsional Buckling of Wooden Beams with Mid-span Lateral Bracing offset from Section Mid-height

by Ye Hu[1], Magdi Mohareb[2], Member, ASCE, and Ghasan Doudak[3], Member, ASCE

[1] Research Assistant, Dept. of Civil Engineering, University of Ottawa, Ottawa, ON, Canada, K1W6N5. Email: yhu005@uottawa.ca
[2]Professor, Dept. of Civil Engineering, University of Ottawa, Ottawa, ON, Canada, K1W6N5 (corresponding author). Email: mmohareb@uottawa.ca
[3]Associate Professor, Dept. of Civil Engineering, University of Ottawa, Ottawa, ON, Canada, K1W6N5. Email: gdoudak@uottawa.ca

Abstract:

An energy-based solution is developed for the lateral torsional buckling analysis of wooden beams with a mid-span lateral brace subjected to uniformly distributed loads or mid-span point load. The predicted critical moments and mode shapes are shown to agree with results based on three-dimensional finite element analysis. The study indicates that such beams are prone to two buckling patterns: a symmetric mode and an anti-symmetric mode. Whether the symmetric or the anti-symmetric mode governs the critical moment capacity is shown to depend on the bracing height. A technique is then developed to determine the threshold bracing height required to maximize the critical moment. A parametric study is then conducted to investigate the effect of lateral bracing and load height effects on the critical moments. Simple design equations are developed to predict critical moments for a practical range of cases. The limitations of the simplified procedure are discussed. For cases outside the scope of the simplified procedure, designers are recommended to adopt the more detailed energy-based solution. Design examples are provided to illustrate the merits and applicability of the proposed procedure in practical situations.

Keywords

Lateral torsional buckling, lateral bracing, load height, bracing height, simplified design equations

This article is to be cited as
Hu Y, Mohareb M, Doudak G (2017) Lateral Torsional Buckling of Wooden Beams with Midspan Lateral Bracing Offset from Section Mid-height, Journal of Engineering Mechanics, 143(11) - 04017134

The copy-edited of this article is available at https://doi.org/10.1061/(ASCE)EM.1943-7889.0001359

Introduction and Literature review

Design standards (e.g., CAN-CSA-O86 2014, NDS 205) recognize lateral torsional buckling (LTB) as a failure mode potentially governing the capacity of long span laterally unsupported wood beams. The phenomenon has been experimentally documented (e.g., Hooley and Madsen, 1964 and Xiao, 2014). The LTB resistance of such beams is known to be influenced by the load height effect and by the presence of lateral bracing provided by adjoining members. In practical design, such beams may be laterally restrained at mid-span with braces offset from the section mid-height. Lateral restraints would typically be placed at the top face by means of secondary beam elements, blocking and/or bracing of closely spaced joist elements, or through diaphragm action. In such details, the lateral restraint at top of the beam braces the compression face (when subjected to downwards vertical loading) is consistent with the understanding that it optimizes the LTB capacity of the member. There are cases however that deviate from this convention, including the design of beams for wind uplift, where lateral braces located at beam top would provide bracing near the tension side of the member (Du et al. 2016a, 2016b). A similar situation arises for beam-columns on the leeward side of a building. Additionally, situations arise where the load height and the bracing height may coincide. When such details are encountered, it becomes difficult for the designer to assess the beneficial contribution of the brace on the lateral torsional buckling capacity. Currently, there are no provisions in design standards (CAN-CSA O86 2014, NDS 2015) that address such cases, and the present study provides a model and a simple expression to aid the designer in evaluating whether a lateral brace offset from the compression face or the neutral axis can be considered to optimize the resistance for LTB failure.

Wood design recommendations (e.g., AFPA 2003) and structural steel standards (e.g., CAN-CSA S16 2014, AS4100 1998, Eurocode 2005, AISC 2010) account for the effect of load height and

presence of lateral bracing systems, either through the effective length approach, the equivalent moment factor approach, or other approximate methods. However, no recommendations are provided to account for the influence of bracing heights. Within this context, the present study investigates the combined effect of load height and bracing height on the lateral torsional buckling capacity of simply supported wood beams.

Load height effect

The load height effect on lateral torsional buckling has been heavily investigated for steel beams and, to a limited extent, for wood beams. The present review covers both types of applications given their mechanistic commonalities. It is cautioned however that while gravity loading at the bottom flange is possible in steel beams, such loading is discouraged in wood beams given that it is associated tensile stresses perpendicular to the grain, which could lead to premature failure. Early work includes the work Prescott and Carrington (1920), Timoshenko (1936), Winter (1941), Schrader (1941), Austin et al. (1955), Pettersson et al. (1952). Kerensky et al. (1956) developed a solution that captures the effect of top flange loading for beams by introducing the effective length approach. Nethercot and Rockey (1971) accounted for the load height effect for simply supported beams by introducing design coefficients in critical moment equations. Based on the Rayleigh-Ritz method, JingPing et al. (1988) evaluated the inelastic LTB capacity of beam-columns subjected to two symmetric transverse loads. Helwig et al. (1997) and Samanta and Kumar (2006) investigated the load height effect by conducting a shell-based finite element analysis (FEA) for mono-symmetric beams. A few studies investigated cases involving top flange, mid-height and bottom flange loading: Yura et al. (2008) developed an expression for the elastic critical moment for twin girders with doubly symmetric and singly symmetric cross sections. White and Kim (2008) conducted experiments to verify LTB predictions in AASHTO (2004) and AISC (2005).

Mohebkhah (2010) developed an FEA model to investigate inelastic LTB capacity of simply supported I-beams. Wong et al. (2015) compared previous design recommendations with experimental results of White and Kim (2008) and extended the effective length factor concept to a variety of loading scenarios for simply supported beams. While the above studies were primarily aimed at examining the load height effect on LTB resistance, the topic has been partly investigated in various investigations such as Ings and Trahair (1987), Pi et al. (1992), Andrade and Camotim (2005), Mohri and Potier-Ferry (2006), Andrade et al. (2007), Erkmen and Mohareb (2008), Wu and Mohareb (2010), Trahair (2013), Lamb and Eamon (2015), Sahraei et al. (2015), and Sahraei and Mohareb (2016). A common observation in the above studies is that the elastic and inelastic LTB resistances for beams decrease as the point of application of loads induced by gravity moves upwards.

Lateral restraint effect

The effect of continuous rigid lateral top-flange bracing on the LTB analysis of simply supported beams was investigated by Park et al. (2004) by developing a FEA model. A comparison of the results has shown that the moment gradient factor equation of Yura (1993) leads to un-conservative results for uniformly distributed loads. For such cases, Park et al. (2004) proposed supplementary design equations. Samanta and Kumar (2008) developed a FEA model for the LTB analysis of mono-symmetric cantilever I-beams with three types of rigid lateral braces at top flange, bottom flange, and both flanges. For long span beams, top flange bracing was found to be more effective than bottom flange bracing and corresponded to a significant increase in buckling capacity. Bracing both flanges was reported to be most effective in increasing the LTB capacity. For short span beams, lateral bracing at top and bottom flanges was found to be only moderately effective.

106 Several experimental and analytical studies have investigated the effect of flexible lateral restraint
107 on the LTB capacity (e.g. Flint, 1951). In the above studies, top flange lateral bracing was observed
108 to significantly increase the LTB resistance of beams when compared to shear centre or bottom
109 flange bracing.
110 Only a few studies investigated the combined effect of load height and lateral bracing height.
111 Schmidt (1965) analytically and numerically investigated the LTB of beams with central lateral
112 bracing subjected to mid-span point loading. The lateral bracing point coincided with the loading
113 point and both were assumed to be offset from the shear centre. Kitipomchai et al. (1984)
114 investigated the LTB of cantilever I-beams with offset intermediate restraint and vertical loads.
115 Wang et al. (1987) numerically determined the LTB capacity of mono-symmetric cantilevers with
116 eccentric vertical loading and discrete lateral bracing offset from the shear centre. Both studies
117 (Kitipomchai, 1984 and Wang et al., 1987) did not specifically address the benefits of bracing
118 height. McCann et al. (2013) investigated simply supported beams with doubly symmetric I
119 sections subjected to uniform moments with discrete equally spaced eccentric linearly elastic
120 braces. In the study, the lateral bracing point was assumed to coincide with the loading point and
121 the warping effect was omitted. The study did not investigate the load height effect. Within this
122 context, the present study investigates the combined effect of bracing height and load height on
123 the elastic LTB capacity of wooden beams with emphasis on: (a) developing a mathematical model
124 able capture the important characteristics of the solution, (b) investigating the effect of bracing
125 height on the LTB capacity and mode shapes, (c) conducting a parametric study to investigate the
126 effects of key parameters on the LTB resistance, and (d) developing simplified equations for
127 bracing height requirement and corresponding critical moments.

Statement of the Problem

A wooden beam with a doubly symmetric cross-section is simply supported relative to the vertical and lateral displacements and twist at both ends. The beam is subjected to a reference distributed load $q(z)$ offset from the section mid-height axis by a height a taken as positive when the load is above the section mid-height. A mid-span lateral brace offset from the section mid-height is provided at a height b taken as positive when above the section mid-height (Fig. 1). The reference loads $q(z)$ are assumed to increase to reach a critical value $\lambda q(z)$ where the system becomes in a neutral state of stability, at which it has a tendency to undergo lateral torsional buckling without further increase in loading. It is required to determine the critical load magnitude $\lambda q(z)$ at the onset of buckling.

Assumptions

The following assumptions are made

1. The material is linearly elastic and orthotropic. Given that properties of wood in the tangential and radial directions are nearly equal (FPL, 2010), the nine orthotropic constitutive constants are shown to reduce to six (Xiao 2014). A sensitivity study based on a 3D finite element buckling analysis (Xiao et al. 2014) has shown that the elastic lateral buckling resistance of beams is influenced only by two constitutive properties: the longitudinal Young's modulus E and the shear modulus G for shear stresses acting on the normal plane. The study has shown that changing the remaining material properties by +/-50% influence the predicted critical moments by less than 1%.Thus, the present study characterizes the constitutive behaviour of wood using only constants E and G in a manner similar to isotropic materials.
2. Load distribution is symmetric about the beam mid-span.

3. The direction of applied load is constant (i.e., conservative loading), and

4. Cross-sectional distortions and shear deformations are negligible

Formulation

Variational Principle

The total potential energy $\pi = U + V$ is the summation of the internal strain energy U and the load potential energy gained V. The internal strain energy U is given by (e.g., Trahair 1993)

$$U = \frac{1}{2}\int_0^L EI_{yy}u''^2 dz + \frac{1}{2}\int_0^L GJ\theta'^2 dz + \frac{1}{2}\int_0^L EC_w\theta''^2 dz \quad (1)$$

where $u = u(z)$ is lateral displacement, $\theta = \theta(z)$ is the twist angle, both being functions of the longitudinal coordinate z, L is the span, E is Young's modulus, I_{yy} is the weak moment of inertia, G is shear modulus, J is the Saint-Venant torsional constant, and C_w is the warping constant. The load potential energy gained by the load V consists of two components $V = V_1 + V_2$ and is given by (e. g., Trahair 1993)

$$V_1 = \lambda\int_0^L M(z)\theta u'' dz, \quad V_2 = -\frac{\lambda}{2}\int_0^L q(z)a\theta^2 dz \quad (2)\text{a,b}$$

where V_1 is the load potential energy gained by the strong axis bending moments $M = M(z)$ induced by the transverse loads, undergoing lateral displacements $u(z)$ and angle of twist $\theta(z)$ and V_2 is the load potential gained by the distributed load $q(z)$ acting at a distance a above the section mid-height undergoing an angle of twist $\theta(z)$ and λ is a load multiplier to determined based on a buckling analysis.

Assumed Displacement Functions

The displacement functions are assumed to take the form

$$u(z)=\left(\sum_{i=1}^{2n} A_i \sin\frac{i\pi z}{L}\right)+A_{2n+1}\sin\frac{(2n+1)\pi z}{L},\ \theta(z)=\sum_{j=1}^{2n} B_j \sin\frac{j\pi z}{L} \qquad (3),(4)$$

The above displacement functions meet the essential and natural boundary conditions $u(0)=u''(0)=u(L)=u''(L)=0$ and $\theta(0)=\theta''(0)=\theta(L)=\theta''(L)=0$. The presence of a mid-span lateral brace at a height b above section mid-height provides a kinematic constraint between the displacement $u(L/2)$ and the angle of twist $\theta(L/2)$ at beam mid-span. From Fig. 2, one obtains the kinematic constraint $u(L/2)=-\theta(L/2)b$. From Eqs. (3) and (4) by setting $z=L/2$, and substituting into the kinematic constraint equation, one can express constant A_{2n+1} in terms of the remaining constants A_i, B_i ($i=1,..n$) as $A_{2n+1}=-\sum_1^{2n}(-1)^n\left(A_i+bB_i\right)\sin(i\pi/2)$. Then, from the expression for A_{2n+1}, by substituting into Eq.(3), one obtains

$$u(z)=\sum_{i=1}^{2n} A_i\left[\sin\frac{i\pi z}{L}+(-1)^{n+1}\sin\frac{i\pi}{2}\sin\frac{(2n+1)\pi z}{L}\right]+b\sum_{i=1}^{2n} B_i(-1)^{n+1}\sin\frac{i\pi}{2}\sin\frac{(2n+1)\pi z}{L} \qquad (5)$$

Internal Strain Energy

From Eqs. (4) and (5), by substituting into the internal strain energy expression given in Eq.(1), one obtains

$$U=\frac{1}{2}\left\langle \mathbf{A_a}^{\mathrm{T}} \quad \mathbf{A_b}^{\mathrm{T}} \right\rangle \begin{bmatrix} \mathbf{k}_1 & \mathbf{0} \\ \mathbf{0} & \mathbf{k}_2 \end{bmatrix} \begin{Bmatrix} \mathbf{A}_{\mathrm{a}} \\ \mathbf{A}_{\mathrm{b}} \end{Bmatrix} \qquad (6)$$

where

$$\mathbf{A}_{\mathrm{a}\ 1\times 2n}^{\mathrm{T}} = \begin{pmatrix} A_2 & B_2 & A_4 & B_4 & \cdots & A_{2n} & B_{2n} \end{pmatrix}, \mathbf{A}_{\mathrm{b}\ 1\times 2n}^{\mathrm{T}} = \begin{pmatrix} A_1 & B_1 & A_3 & B_3 & \cdots & A_{2n-1} & B_{2n-1} \end{pmatrix},$$

185
$$\mathbf{k}_1 = \begin{bmatrix} \mathbf{m}_{1,1} & \mathbf{m}_{1,3} & \cdots & \mathbf{m}_{1,2i-1} & \cdots & \mathbf{m}_{1,2n-1} \\ \mathbf{m}_{3,1} & \mathbf{m}_{3,3} & \cdots & \mathbf{m}_{3,2i-1} & \cdots & \mathbf{m}_{3,2n-1} \\ \vdots & \vdots & \ddots & \vdots & \iddots & \vdots \\ \mathbf{m}_{2j-1,1} & \mathbf{m}_{2j-1,3} & \cdots & \mathbf{m}_{2j-1,2i-1} & \cdots & \mathbf{m}_{2j-1,2n-1} \\ \vdots & \vdots & \iddots & \vdots & \ddots & \vdots \\ \mathbf{m}_{2n-1,1} & \mathbf{m}_{2n-1,3} & \cdots & \mathbf{m}_{2n-1,2i-1} & \cdots & \mathbf{m}_{2n-1,2n-1} \end{bmatrix}, \mathbf{k}_2 = \begin{bmatrix} \mathbf{m}_{2,2} & \mathbf{m}_{2,4} & \cdots & \mathbf{m}_{2,2i} & \cdots & \mathbf{m}_{2,2n} \\ \mathbf{m}_{4,2} & \mathbf{m}_{4,4} & \cdots & \mathbf{m}_{4,2i} & \cdots & \mathbf{m}_{4,2n} \\ \vdots & \vdots & \ddots & \vdots & \iddots & \vdots \\ \mathbf{m}_{2j,2} & \mathbf{m}_{2j,4} & \cdots & \mathbf{m}_{2j,2i} & \cdots & \mathbf{m}_{2j,2n} \\ \vdots & \vdots & \iddots & \vdots & \ddots & \vdots \\ \mathbf{m}_{2n,2} & \mathbf{m}_{2n,4} & \cdots & \mathbf{m}_{2n,2i} & \cdots & \mathbf{m}_{2n,2n} \end{bmatrix}$$

186
$$\mathbf{m_{j,i}} = \begin{bmatrix} m_{1,i,j} & 0 \\ 0 & m_{3,i,j} \end{bmatrix} + b \begin{bmatrix} 0 & m_{2,i,j} \\ m_{2,i,j} & 0 \end{bmatrix} + b^2 \begin{bmatrix} 0 & 0 \\ 0 & m_{4,i,j} \end{bmatrix} \tag{7}$$

187
$$\begin{aligned} m_{1,i,j} &= EI_{yy} \left[\left(\frac{i\pi}{L} \right)^2 \left(\frac{j\pi}{L} \right)^2 \int_0^L \sin \frac{i\pi z}{L} \sin \frac{j\pi z}{L} dz + \frac{L}{2} \sin \frac{i\pi}{2} \sin \frac{j\pi}{2} \left(\frac{(2n+1)\pi}{L} \right)^4 \right] \\ m_{2,i,j} &= \frac{L}{2} EI_{yy} \sin \frac{i\pi}{2} \sin \frac{j\pi}{2} \left(\frac{(2n+1)\pi}{L} \right)^4 \\ m_{3,i,j} &= GJ \left(\frac{i\pi}{L} \right) \left(\frac{j\pi}{L} \right) \int_0^L \cos \frac{i\pi z}{L} \cos \frac{j\pi z}{L} dz + EC_w \left(\frac{i\pi}{L} \right)^2 \left(\frac{j\pi}{L} \right)^2 \int_0^L \sin \frac{i\pi z}{L} \sin \frac{j\pi z}{L} dz \\ m_{4,i,j} &= \frac{L}{2} EI_{yy} \sin \frac{i\pi}{2} \sin \frac{j\pi}{2} \left(\frac{(2n+1)\pi}{L} \right)^4 \end{aligned} \tag{8}$$

188 **Fourier Expansion of bending moments:**

189 A given bending moment $M(z)$ can be expressed in a Fourier series as

190
$$M(z) = \sum_{k=1,2}^{kmax} m_k \sin \frac{k\pi z}{L} \qquad m_k = \frac{2}{L} \int_0^L M(z) \sin \frac{k\pi z}{L} dz \tag{9)a,b}$$

191 For the case of a mid-span load, the moment distribution is given by

192 $\lambda M(z) = \lambda Q z / 2, \quad 0 \le z \le L/2$ and $\lambda M(z) = \lambda Q(L - z) / 2, 0 \le z \le L/2$. By substituting into Eq.

193 (9)b, one obtains $m_k = 2QL / k^2 \pi^2, (k = 1,3,5\ldots)$. For the case of a uniformly distributed load λq,

194 the bending moment expression takes the form $\lambda M(z) = \lambda q (Lz - z^2) / 2$. Using the Fourier

195 expansion in Eq.(9), one obtains the Fourier coefficients $m_k = 4\lambda q L^2 / (k\pi)^3 \qquad (k = 1,3,5\ldots)$

Destabilizing term due to bending moments

For symmetric loading, it can be demonstrated (Appendix A) that the destabilizing term due to bending moments takes the form

$$V_1 = \frac{\lambda}{2}\left\langle \mathbf{A}_a{}^T \quad \mathbf{A}_b{}^T \right\rangle \begin{bmatrix} \mathbf{k}_{g1} & \mathbf{0} \\ \mathbf{0} & \mathbf{k}_{g2} \end{bmatrix} \begin{Bmatrix} \mathbf{A}_a \\ \mathbf{A}_b \end{Bmatrix} \tag{10}$$

while that the due to load height effect takes the form

$$V_2 = \frac{\lambda}{2}\left\langle \mathbf{A}_a{}^T \quad \mathbf{A}_b{}^T \right\rangle \begin{bmatrix} \mathbf{k}_{g3} & \mathbf{0} \\ \mathbf{0} & \mathbf{k}_{g4} \end{bmatrix}_{(i)} \begin{Bmatrix} \mathbf{A}_a \\ \mathbf{A}_b \end{Bmatrix} \tag{11}$$

where the entries of the geometric sub-matrices $\mathbf{k}_{g1}$, $\mathbf{k}_{g2}$, $\mathbf{k}_{g3(i)}$ $\mathbf{k}_{g4(i)}$ are provided in Appendix A for the cases of mid-span point load $i = 1$ and for the case of uniformly distributed load $i = 2$.

Stationarity conditions

From Eqs. (6), (10), and (11), by substituting into $\pi = U + V_1 + V_2$, and evoking the stationarity conditions $\partial\pi/\partial\mathbf{A}_a = \partial\pi/\partial\mathbf{A}_b = \mathbf{0}$, one obtains

$$\left\{ \begin{bmatrix} \mathbf{k}_1 & \mathbf{0} \\ \mathbf{0} & \mathbf{k}_2 \end{bmatrix} + \lambda \left(\begin{bmatrix} \mathbf{k}_{g1} & \mathbf{0} \\ \mathbf{0} & \mathbf{k}_{g2} \end{bmatrix} + \begin{bmatrix} \mathbf{k}_{g3} & \mathbf{0} \\ \mathbf{0} & \mathbf{k}_{g4} \end{bmatrix} \right) \right\} \begin{Bmatrix} \mathbf{A}_a \\ \mathbf{A}_b \end{Bmatrix} = 0 \tag{12}$$

The two partitions of Eq. (12) can be expanded to yield

$$\left(\mathbf{k}_1 + \lambda \left(\mathbf{k}_{g1} + \mathbf{k}_{g3} \right) \right) \mathbf{A}_a = \mathbf{0} \tag{13}$$

$$\left(\mathbf{k}_2 + \lambda \left(\mathbf{k}_{g2} + \mathbf{k}_{g4} \right) \right) \mathbf{A}_b = \mathbf{0} \tag{14}$$

The non-trivial solution of Eq. (12) is given by setting the determinant of the matrix of coefficients to zero, i.e.,

213 $$\begin{vmatrix} \mathbf{k}_1 + \lambda\left(\mathbf{k}_{g1} + \mathbf{k}_{g3}\right) & \mathbf{0} \\ \mathbf{0} & \mathbf{k}_2 + \lambda\left(\mathbf{k}_{g2} + \mathbf{k}_{g4}\right) \end{vmatrix} = 0$$

214

215 The above determinant identity is equivalent to $\left|\mathbf{k}_1 + \lambda\left(\mathbf{k}_{g1} + \mathbf{k}_{g3}\right)\right| \times \left|\mathbf{k}_2 + \lambda\left(\mathbf{k}_{g2} + \mathbf{k}_{g4}\right)\right| = 0$ which

216 is satisfied either when the conditions $\left|\mathbf{k}_1 + \lambda\left(\mathbf{k}_{g1} + \mathbf{k}_{g3}\right)\right| = 0$ or $\left|\mathbf{k}_2 + \lambda\left(\mathbf{k}_{g2} + \mathbf{k}_{g4}\right)\right| = 0$ are

217 satisfied. If the eigen-value $\lambda = \lambda_1$ satisfies the first condition $\left|\mathbf{k}_1 + \lambda\left(\mathbf{k}_{g1} + \mathbf{k}_{g3}\right)\right| = 0$, Eq. (13)

218 indicates that $\mathbf{A}_a \neq \mathbf{0}$. In this case, the condition $\left|\mathbf{k}_2 + \lambda_1\left(\mathbf{k}_{g2} + \mathbf{k}_{g4}\right)\right| = \mathbf{0}$ will, in general, be

219 violated indicating that the only solution of Eq. (14) is $\mathbf{A}_b = \mathbf{0}$. In a similar manner, if the eigen-

220 value $\lambda = \lambda_2$ satisfies the condition $\left|\mathbf{k}_2 + \lambda\left(\mathbf{k}_{g2} + \mathbf{k}_{g4}\right)\right| = 0$, Eq. (14) indicates that $\mathbf{A_b} \neq \mathbf{0}$ and the

221 condition $\left|\mathbf{k}_1 + \lambda_2\left(\mathbf{k}_{g1} + \mathbf{k}_{g3}\right)\right| = 0$ will, in general, be violated indicating that $\mathbf{A}_a = \mathbf{0}$. It is noted

222 that the entries of vector $\mathbf{A}_a$ always correspond to a symmetric buckling mode while the

223 coefficients of vector $\mathbf{A}_b$ correspond to an anti-symmetric mode (Hu 2016).

224 In summary, the solution for the eigen-value problem in Eq. (12) has two sets of possible eigen

225 values: The first set $\lambda = \lambda_1$ arises from the solution of the condition $\left|\mathbf{k}_1 + \lambda_1\left(\mathbf{k}_{g1} + \mathbf{k}_{g3}\right)\right| = 0$ and

226 the corresponding eigen-vectors are $\mathbf{A}_a \neq \mathbf{0}$, $\mathbf{A}_b = \mathbf{0}$. The second set $\lambda = \lambda_2$ arises from the

227 solution of $\left|\mathbf{k}_2 + \lambda_2\left(\mathbf{k}_{g2} + \mathbf{k}_{g4}\right)\right| = \mathbf{0}$ and the corresponding eigen vectors are $\mathbf{A}_a = \mathbf{0}$ and $\mathbf{A_b} \neq \mathbf{0}$.

228 For the special case where both conditions $\left|\mathbf{k}_1 + \lambda\left(\mathbf{k}_{g1} + \mathbf{k}_{g3}\right)\right| = 0$ and $\left|\mathbf{k}_2 + \lambda\left(\mathbf{k}_{g2} + \mathbf{k}_{g4}\right)\right| = 0$ are

229 satisfied, one has a repeated eigenvalue $\lambda_1 = \lambda_2$. In such a case Equations (13) and (14) indicate

that the conditions $\mathbf{A}_a \neq \mathbf{0}$ and $\mathbf{A}_b \neq \mathbf{0}$ are possible. Such a case is treated in detail in the section titled "Recovering the threshold bracing height".

Recovering the threshold bracing height

As shown in the results (e.g., Fig. 6), while the critical load corresponding to Mode 1 (symmetric) depends on the bracing height, that based on Mode 2 (anti-symmetric) is independent of it, yielding a constant critical moment value for a given beam geometry and load configuration. In contrast, the buckling moment corresponding to Mode 1 decreases as the bracing height is lowered. Conceptually, there is a threshold bracing height b_{cr} at which both modes yield the same critical moments. When the brace is above this threshold height, the member attains its maximal capacity as dictated by the anti-symmetric mode. The present section develops a methodology to recover the critical bracing height: Equation (14) is solved for the eigenvalue λ_2 , and one sets $\lambda_1 = \lambda_2$. Equation (13) is then solved for the threshold bracing height b_{cr}. From Eqs. (7), the elastic stiffness matrix $\mathbf{k}_1$ can be re-written as the sum of three matrices

$$\mathbf{k}_1 = \bar{\mathbf{k}}_1 + b_{cr}\bar{\bar{\mathbf{k}}}_1 + b_{cr}^2\bar{\bar{\bar{\mathbf{k}}}}_1 \tag{15}$$

where matrices $\mathbf{k}_1, \bar{\bar{\mathbf{k}}}_1, \bar{\bar{\bar{\mathbf{k}}}}_1$ are provided in Appendix B

Also, from Eq.(25), the geometric stiffness matrix $\mathbf{k}_{g1}$ can be expressed as

$$\mathbf{k}_{g1} = \bar{\mathbf{k}}_{g1} + b_{cr}\bar{\bar{\mathbf{k}}}_{g1} \tag{16}$$

and matrices $\bar{\mathbf{k}}_{g1}, \bar{\bar{\mathbf{k}}}_{g1}$ are provided in Appendix B. From Eqs. (15) and (16), by substituting into Eq. (13), one obtains a quadratic eigenvalue problem in the unknown critical bracing height b_{cr}

$$\left[\left(\overline{\mathbf{k}}_1+\lambda_2\overline{\mathbf{k}}_{g1}+\lambda_2\mathbf{k}_{g3}\right)+b_{cr}\left(\overline{\overline{\mathbf{k}}}_1+\lambda_2\overline{\overline{\mathbf{k}}}_{g1}\right)+b_{cr}^2\overline{\overline{\overline{\mathbf{k}}}}_1\right]\mathbf{A}_a=\mathbf{0} \quad (17)$$

Given λ_2, one can recover the sought critical bracing height by solving the quadratic eigen value problem defined in Eq. (17).

Verification Example

To verify the validity of the model, the critical moments of a reference beam as predicted by the present model are compared to those based on a 3D FEA eigen-value buckling analyses based on the commercial software ABAQUS for various bracing heights. The reference beam has a width $w=130mm$, a height $h=950mm$ and a span of $13,000mm$. For a rectangular section of width w and depth h, $I_{yy}=hw^3/12=1.74\times10^8 mm^4$, $C_w=w^3h^3/144=1.31\times10^{13}mm^6$ and the Saint-Venant torsional constant as given in the detailed method of Pai (2007) is $J=6.36\times10^8 mm^4$. Material is assumed to be glued-laminated timber, Spruce-Lodgepole Pine with 20f-EX grade. The modulus of elasticity in the longitudinal direction is taken as $E=E_L=10,300MPa$ (CSA O86 2014) and shear modulus is $G=G_{LT}=G_{LR}=474MPa$ (FPL 2010).

Convergence study of present model

To determine the number of Fourier terms *n* needed for convergence, a convergence study was conducted on 20 cases with different load configurations (uniformly distributed, mid-span point loads), brace heights $b/h=-0.5,0.0,0.5$ and load heights $a/h=-0.5,0.0,0.5$. Detailed descriptions and results from the convergence study can be found in (Hu 2016). The ratio of critical moments based on $n=4$ to those based on $n=6$ where shown to be less than 0.63% in all 20 cases considered. Given that the computational time involved is nearly instantaneous, the number of modes n was conservatively set to 9 in subsequent runs, (i.e., 18 Fourier terms were taken in Eqs. (3) and (4)).

The 3D finite element model

The C3D8 brick element in ABAQUS was used to discretize the beam. The C3D8 element is three-dimensional continuum elements in ABAQUS consisting of 8 nodes at the corners and 24 degrees of freedom in total (three translations at each node) (Simulia, 2011). This type of element uses linear interpolation in each direction. An orthotropic material model is adopted to represent the wood properties. In a manner consistent with the work of Xiao (2014) and Xiao et al. (2014), the modulus of elasticity in the longitudinal direction is taken as $E_L = 10300MPa$ and the moduli of elasticity in the tangential and radial directions were taken as $E_T = E_R = 700MPa$. The shear moduli are taken as $G_{LR} = G_{LT} = 474MPa$ and $G_{RT} = 51.5MPa$ and the Poisson's ratios are taken as $\nu_{LR} = \nu_{LT} = 0.347$ and $\nu_{RT} = 0.469$. To simulate simply supported boundary conditions at both ends relative to pre-buckling transverse displacements (i.e., $v(0) = v(L) = 0$) and bucking twist and lateral deflections (i.e., $u(0) = \theta(0) = u(L) = \theta(L) = 0$) while keeping free the strong axis rotations $v'(0) \neq 0, v'(L) \neq 0$, weak axis rotations, and warping deformations $\theta'(0) \neq 0, \theta'(L) \neq 0$ in a manner consistent with the model developed in the present study, two groups of restraints were enforced at both ends of the model: (1) As shown in Fig. 3, a set of constraints related to vertical displacements were imposed along axes AB and $A'B'$ at the end cross sections. For axes CD and $C'D'$, the lateral displacements were restrained by imposing another group of constraints. (2) The centroid of the cross section at one end was longitudinally restrained (Fig.3a), while that at the other end was left free to move longitudinally (Fig.3b). The mid-span lateral brace was simulated by retraining the lateral displacement at the node located at the target bracing height on the mid-span vertical line passing through the section centroid. A mesh sensitivity analysis was conducted on 12 cases with different load configurations (uniformly

294 distributed, mid-span point loads), brace heights $b/h = -0.5, 0.0, 0.5$ and load heights
295 $a/h = -0.5, 0.0, 0.5$. The governing modes were symmetric in some of the runs and anti-symmetric
296 in other runs. The results (Hu 2016) showed that critical moment predictions based on 410
297 elements longitudinally, 50 elements along the height, 10 elements along the width do not change
298 by more than 0.08% when finer meshes are taken. Thus, a 410x50x10 mesh will be taken in
299 subsequent runs.

300 **Comparison of critical moments and buckling modes**

301 Three sets of comparisons were conducted by varying bracing height with different load height
302 cases (i.e. top face, mid-height, and bottom face) between the results of formulation developed in
303 the present study and those based on the ABAQUS model. The buckling load magnitudes obtained
304 from the two solutions are overlaid in Fig. 4. Both models predict two types of buckling modes:
305 symmetric and anti-symmetric. The anti-symmetric mode is associated with a critical moment
306 value that is independent of the bracing height while critical moment based on the symmetric mode
307 is found to depend on the bracing height. Fig. 4 shows close agreement between the predictions of
308 the present study and those of the ABAQUS simulations. Percentage differences were found to be
309 within 1.09%-4.08% (Hu 2016). The buckling load values obtained from the present study are
310 slightly higher than those obtained from the ABAQUS simulation. The difference is due to the fact
311 that the present model is based on the simplifying kinematic assumptions that neglect distortional
312 and shear deformation effects and thus provides a slightly higher representation of the beam
313 stiffness than the ABAQUS model which allows distortion and shear deformations effects. The
314 symmetric and anti-symmetric buckling modes are compared to ABAQUS 3D results (Fig. 5) for
315 the cases of point load and uniformly distributed load for the cases

316 $(a/h, b/h) = (0,0), (0.5,0), (0,0.5), (0.5,0.5)$. Close agreement is observed between the present
317 model and those based on the ABAQUS simulations.

318 **Parametric study**

319 A parametric study was conducted by varying the bracing height and load heights (i.e. top face,
320 mid-height and bottom face) for point load and uniformly distributed load cases (Fig. 6). The
321 buckling load corresponding to the anti-symmetric mode (Mode 2) is observed to be independent
322 of the bracing height. For both loading cases, the buckling load for Mode 1 decreases when the
323 lateral brace is moved downwards. Also, for both loading cases, the buckling load corresponding
324 Mode 1 decreases with load height increase. For Mode 2, the buckling load is observed to be
325 independent of load height for the case of point load but found to decrease with load height increase
326 for the case of uniformly distributed load.

327 **Development of Simplified design expressions**

328 A database of 148 runs (Hu 2016) was developed to investigate the effect of various geometric
329 and elastic properties on threshold bracing height and the critical moment. Of the 148 cases, 68
330 runs investigated the case of point load and 80 runs were conducted for the case of uniformly
331 distributed load. Ranges of material properties were chosen to conform to those provided in CSA
332 O86 (2014) and (FPL, 2010). The ranges of parameters investigated are $0.137 \le w/h \le 0.856$,
333 $8.42 \le L/h \le 21.05$, and $1/10 \le G/E \le 1/20$. Subsequently, approximate design expressions were
334 developed based on regressing analysis.

Point load

The relationship between the critical bracing height to section height ratio $\bar{b}_{cr}/h$ and the parameters $w/h, L/h, a/h, G/E$ were found to exhibit a nearly linear dependence (Hu 2016). Therefore, the approximate critical height ratio $\bar{b}_{cr}/h$ was postulated to take the form

$$\left(\frac{\bar{b}_{cr}}{h}\right) \approx \alpha_0 + \alpha_1\left(\frac{w}{h}\right) + \alpha_2\left(\frac{L}{h}\right) + \alpha_3\left(\frac{a}{h}\right) + \alpha_4\left(\frac{G}{E}\right) \tag{18}$$

where $\alpha_0, \alpha_1, \alpha_2, \alpha_3, \alpha_4$ are coefficients to be determined from the regression analysis. The sum of the squares of the differences between the values of $\left(b_{cr}/h\right)$ as obtained by the present solution and that based on the expression in Eq. (18) is minimized, i.e.,

$$D_1 = \sum_{i=1}^{m}\left[\left(\frac{\bar{b}_{cr}}{h}\right) - \left(\frac{b_{cr}}{h}\right)\right]_i^2 = \min \tag{19}$$

where m is the number of runs conducted, by enforcing the minimization conditions $\partial D_1/\partial \alpha_i = 0 \quad (i = 0,1..4)$ yielding the regression constants $\alpha_0 = 0.08089, \alpha_1 = 0.07364$, $\alpha_2 = -0.01529, \alpha_3 = 0.6870, \alpha_4 = -1.5130$. The domain validity of the regression coefficients is that of the database of runs, i.e., $0.137 \le w/h \le 0.856, 8.42 \le L/h \le 21.05$, and $1/10 \le G/E \le 1/20$. Within these domains, the standard deviation of the difference between the predictions of the regression equation $\bar{b}_{cr}/h$ to that of the present solution was found to be 0.0041. When the bracing height b is greater than the critical bracing height b_{cr} (or $\bar{b}_{cr}$ as estimated by Eq.(18)), the critical moment will be maximized and will attain that based on the anti-symmetric mode. Under this mode, the lateral displacement and angle of twist vanish at beam mid-span and the unsupported length is $L_u = L/2$. The corresponding critical moment M_{cr} is then given by

354 $$\bar{M}_{cr} \approx C_b \frac{\pi}{L_u}\sqrt{EI_{yy}GJ + \left(\frac{\pi E}{L_u}\right)^2 I_{yy}C_w} \qquad (20)$$

355 where C_b is a moment gradient factor within the beam half-span. Given the critical moment values
356 M_{cr} based on the present analysis (Hu 2016) and knowing E , I_{yy}, G , J , C_w and L_u , the moment
357 gradient factor C_b is determined for each run. The procedure was repeated for all 68 runs and was
358 found to range from 1.78 to 1.81 with an average value of 1.80 and a standard deviation of 0.008.
359 The value $C_b = 1.80$ obtained is in line with that based on quarter point formulas of the AFPA
360 (2003) of 1.67, CAN-CSA S16 (2014) of 1.74, and, AS4100 (1998) of 1.82.

361 **Uniformly distributed load**

362 The approximate critical height ratio $\bar{\bar{b}}_{cr}/h$ was postulated to take the form

363 $$\left(\frac{\bar{\bar{b}}_{cr}}{h}\right) \approx \beta_0 + \beta_1\left(\frac{w}{h}\right) + \beta_2\left(\frac{L}{h}\right) + \beta_3\left(\frac{a}{h}\right) + \beta_4\left(\frac{a}{h}\right)^2 + \beta_5\left(\frac{G}{E}\right) \qquad (21)$$

364 where m is the number of runs conducted (Hu 2016) by enforcing the conditions
365 $\partial D_1/\partial\beta_i = 0 \quad i = 0,1,2..5$ yielding the regression constants $\beta_0 = 0.1740$, $\beta_1 = 0.1368$,
366 $\beta_2 = -0.02950$, $\beta_3 = 0.2944$, $\beta_4 = 0.1595$, $\beta_5 = -2.9995$. The domain validity of the regression
367 coefficients is $0.137 \le w/h \le 0.856$, $-0.5 \le a/h \le 0.5$, $8.42 \le L/h \le 15.79$, $1/10 \le G/E \le 1/20$.
368 Within these domains, the standard deviation of the difference between the predictions of the
369 regression equation $\bar{b}_{cr}/h$ to that of the present solution was found to be 0.0066. When the bracing
370 height is greater than the critical bracing height b_{cr} or $\bar{\bar{b}}_{cr}$ as estimated by Eq. (21), the buckling
371 capacity will be maximized and will attain the critical moment of the anti-symmetric mode. Under
372 this mode, the lateral displacement and angle of twist vanish at mid-span. Under these conditions,

373 the unsupported length is $L_u = L/2$. As the critical moments based on the anti-symmetric mode
374 changes with the load height position (e.g., Fig. 6), additional terms to capture the load height
375 effect should be added to the approximate function. The results of database of runs have shown
376 that the difference between the critical moments for mid-height loading and those based on loading
377 acting at height a above the centroid are nearly proportional to the term aEI_{yy}/L_u^2. As such, the
378 following equation was proposed to estimate the critical moments including load height effects
379 (Hu 2016):

380 $$\bar{\bar{M}}_{cr} = C_b \frac{\pi}{L_u} \sqrt{EI_{yy} GJ + \left(\frac{\pi E}{L_u}\right)^2 I_{yy} C_w} - C_e \frac{aEI_{yy}}{L_u^2} \quad (22)$$

381 The sum of the squares of the differences between the values of the buckling capacity obtained by
382 the present solution (Hu 2016) and that based on (22) is minimized, i.e.

383 $$D_2 = \sum_{i=1}^{m} \left[\bar{\bar{M}}_{cr} - M_{cr} \right]_i^2 = \min \quad (23)$$

384 The minimization process yields the moment gradient factor $C_b = 1.32$ and the load position
385 modifier $C_e = 1.68$. The average value of C_b is consistent with that based on CAN-CSA S16
386 (2014) of 1.32, AFPA (2003) of 1.30, and AS4100 (1998) of 1.33.

387 **Assessment of threshold bracing height predicted by simplified equations**

388 In order to assess the accuracy of the threshold bracing height predictions based on the simplified
389 equations, comparisons are made against 3D FEA results for cases outside the database of runs
390 used to produce the regression results. Two loading cases are considered: mid-span point load and
391 uniformly distributed load. In both cases four loading height are examined:
392 $a/h = -0.25, 0, 0.25, 0.50$. For the point load case, a simply supported glulam beam with a
393 rectangular cross-section of depth $h = 570mm$, width $w = 130mm$ and a span= $11,500mm$ and

sectional and material properties $J = 3.57 \times 10^8 mm^4$, $I_{yy} = 1.04 \times 10^8 mm^4$, $C_w = 2.83 \times 10^{12} mm^6$, $E = 10,300 MPa$ and $G = 515 MPa$. For the uniformly distributed load cases, a simply supported glulam beam with a rectangular cross-section of depth $h = 798 mm$, width $w = 215 mm$ and a span= $10,000 mm$ is taken with sectional and material properties are $J = 2.19 \times 10^9 mm^4$, $I_{yy} = 6.61 \times 10^8 mm^4$, $C_w = 3.51 \times 10^{13} mm^6$, $E = 10,300 MPa$ and $G = 644 MPa$. It is required to determine the threshold bracing height b_{cr}/h in each case based on the simplified expressions and based on ABAQUS. In the case of ABAQUS solution, multiple runs are conducted with different bracing heights in order to identify the threshold bracing height where the symmetric and anti-symmetric modes provide identical critical moments. The results in Table 1 indicate that predictions of both methods agree within 5% of the section height.

Design Example 1- Beam under mid-span point load

A simply supported glulam beam with a rectangular cross-section of depth $h = 570 mm$, width $w = 130 mm$ and a span= $11,500 mm$ is subjected to a mid-span point load acting at top of the cross section. The beam is laterally braced at mid-span. Two bracing heights are considered: (a) $200 mm$ and (b) $0 mm$. Sectional and material properties are $J = 3.57 \times 10^8 mm^4$, $I_{yy} = 1.04 \times 10^8 mm^4$, $C_w = 2.83 \times 10^{12} mm^6$, $E = 10,300 MPa$ and $G = 515 MPa$. It is required to determine the critical moment.

Threshold bracing height check:

For the present problem, one has $w/h = 0.228, L/h = 20.2, a/h = 0.5$ and $G/E = 1/20$. These ratios meet the applicability conditions for Eq.(18). The threshold bracing height ratio as computed from Eq. (18) is $\bar{b}_{cr}/h = 0.057$. This compares to $b_{cr}/h = 0.073$ as predicted by the detailed procedure in Eq. (17), a 0.02 difference. Thus, a bracing height above $0.057 \times 570 = 33 mm$ is deemed high

enough to fully restrain the angle of twist at mid-span and maximize the critical moments by forcing the beam to buckle in an anti-symmetric mode. This condition is satisfied for Case a where the bracing height is $200mm > 33mm$ but not in Case b for a bracing height of $0mm < 33mm$.

Critical moment for case (a)

Since w/h, L/h, a/h, G/E lie within the domain of applicability of the regression equation, the simplified moment calculation in Eq. (20) is applied. As discussed, when twist and lateral displacements vanish at mid-span, the mid-span point is considered as a point of full lateral and torsional restraint and the unbraced length becomes $L_u = L/2 = 5,750mm$. The critical moment $\bar{\bar{M}}_{cr}$ as determined from Eq. (20) is found to be $447kNm$. This value compares to $444kNm$ as predicted by the present formulation, a 0.69% difference, and $437kNm$ as predicted by the 3D ABAQUS model, a 2.23% difference.

Critical moment for case (b)

For zero bracing height, the mid-span section will be only partially restrained from twisting, and the beam capacity will be governed by the symmetric buckling mode. Under this scenario, the critical moment can no longer be calculated using the simplified Eq. (20) and a detailed analysis based on the present formulation would be needed. The critical moment is found to be $M_{cr} = 411kNm$, which compares to $397kNm$ based on the ABAQUS 3D model. As expected, the critical moment is smaller compared to that of Case (a). A lower bound for the critical moment in case (b) can be obtained by entirely omitting the bracing effect at mid-span. Under this scenario, $L_u = L = 11,500mm$ and moment gradient C_b based on the AFPA (2003) recommendations is 1.33. Comparable values are obtained from CAN-CSA S16 (2014) which yields 1.26, or AS4100 (1998) which yields 1.39. For a point load applied at the top of the cross-section, the AFPA (2003)

load eccentricity factor is given by $C_e = \sqrt{\eta^2 + 1} - \eta$ where $\eta = \left(k^* h / 2L_u\right)\sqrt{EI_{yy}/GJ}$ where $k^* = 1.72$ for the case of point loading, yielding $C_e = 0.815$. The sought lower bound of the critical moment is given by $M_{cr} = \left(C_e C_b \pi / L_u\right)\sqrt{EI_{yy}GJ + \left(\pi E / L_u\right)^2 I_{yy} C_w}$ yielding $M_{cr} = 132kNm$. In summary, the critical moment of $411kNm$ based on the detailed procedure is significantly higher than the critical moment based on no intermediate support restraint but slightly less than the critical moment of $444kNm$ based on the case of full bracing.

Example 2 –Beam under a uniformly distributed load

A simply supported glulam beam with rectangular section of depth $h = 798mm$, width $w = 215mm$ is spanning $10,000mm$. The beam is subjected to a uniformly distributed load acting at the top face of the beam. The beam is laterally braced at mid-span. Sectional and material properties are: $J = 2.19 \times 10^9 mm^4$, $I_{yy} = 6.61 \times 10^8 mm^4$, $C_w = 3.51 \times 10^{13} mm^6$, $E = 10,300MPa$ and $G = 644MPa$. Two bracing heights are considered: (a) $100mm$ and (b) $-300mm$ (the negative sign indicates that the bracing is located below the section mid-height). It is required to determine the critical moment capacity.

The dimensionless ratios $w/h = 0.27, L/h = 12.5, a/h = 0.5$ and $G/E = 1/16$ are within the applicability limits of the threshold bracing height and critical moment equations. The threshold bracing height ratio as determined from Eq. (21) is $\bar{\bar{b}}_{cr}/h = -0.158$. This compares to -0.157 based on the detailed procedure, a 0.002 difference. Thus, a bracing height above $-0.158 \times 798 = -126.1mm$ is deemed high enough to fully restrain the angle of twist at mid-span. This happens to be the case for a bracing height of $100mm$ (Case a), but is not for a bracing height of $-300mm$ (Case b). The unbraced length is $L_u = L/2 = 5,000mm$ and the critical moment based

459 on Eq. (22) is found to be $252kNm$. This value compares to $253kNm$ as predicted by the detailed
460 procedure provided, a 0.050% difference.
461 When the bracing height is $-300mm$, the mid-span section will only be partially restrained from
462 twisting and the beam critical moment based on the detailed analysis is found to be $M_{cr} = 171kNm$.
463 As expected, the critical moment is found smaller than that based on Case (a). A lower bound for
464 the critical moment in case (b) can be obtained based on an unsupported length
465 $L_u = L = 10,000mm$ and the moment gradient C_b is determined as 1.13 from the AFPA
466 recommendations (2003), and a load eccentricity factor One can also apply the $C_e = \sqrt{\eta^2 + 1} - \eta$
467 (AFPA 2003) where $\eta = \left(k^* h / 2L_u\right)\sqrt{EI_{yy}/GJ}$ and $k^* = 1.44$ for uniformly distributed load,
468 yielding a value $C_e = 0.779$. The corresponding critical moment is
469 $M_{cr} = \left(C_e C_b \pi / L_u\right)\sqrt{EI_{yy}GJ + \left(\pi E / L_u\right)^2 I_{yy}C_w} = 101kNm$. This lower bound is again significantly
470 lower than the critical moment obtained by the present detailed solution.

471 **Summary and conclusions**

472 Analytical solutions were developed for the lateral torsional buckling analysis of simply supported
473 wooden beams with discrete lateral supports at mid-span subjected to symmetric moment load
474 distributions relative to mid-span. The model accounts for the combined effect of eccentricities of
475 the bracing and the loads. The models were validated against a 3D FEA solutions and parametric
476 study to investigate the influence of mid-span bracing height and load height was conducted. The
477 conclusions can be summarized as follows:
478 1. The model predicts two possible buckling modes: symmetric and anti-symmetric, depending on
479 the load height and bracing height. The anti-symmetric mode in the present study is indirectly
480 promoted by the prescriptive requirements for lumber joists in CAN-CSA O86 (2014) and NDS

(2015) which stipulate cross-bridging or full-height blocking to achieve full twist restraint at the point of brace. Such restraints would suppress the symmetric buckling mode and promote an anti-symmetric buckling mode identical to that obtained in the present study. The present study achieves full twist in a different manner by locating the lateral brace above the critical threshold bracing height.

2. For a given load height, simple expressions were developed for determining the threshold bracing height at which the capacity is governed by the antisymmetric mode.

3. For point load and uniformly distributed load, critical moments based on the symmetric mode are observed to decrease when the load height increases

4. For point load loading, critical moments based on the anti-symmetric modes are found to be independent from the load height. In contrast, for uniformly distributed loads, they are found to decrease as the point of application of the load moves upwards.

5. For mid-span point loading, the threshold bracing height normalized relative to cross section height b_{cr}/h was observed correlate nearly linearly with geometric and elastic parameters a/h, L/h, w/h and G/E.

6. For uniformly distributed loading, the normalized threshold bracing height b_{cr}/h was observed to have a nearly linear correlation with geometric and parameters a/h, w/h and G/E, while having a nearly quadratic correlation with L/h.

7. Simplified design equations were developed to reliably estimate the threshold bracing height required to maximize the critical moments and quantify the critical moments for cases where the bracing location is above the threshold height as computed by the simplified equation.

Appendix A: Formulation of geometric matrices

Destabilizing term due to bending moments

From Eqs.(4), (5) and (9)a, by substituting into Eq. (2)a, one obtains the load potential energy function as

$$V_1 = \frac{\lambda}{2}\left\langle \mathbf{A}_a{}^{T} \quad \mathbf{A}_b{}^{T} \right\rangle \begin{bmatrix} \mathbf{k}_{g1} & \mathbf{k}_{g12}^{T} \\ \mathbf{k}_{g12}^{T} & \mathbf{k}_{g2} \end{bmatrix} \begin{Bmatrix} \mathbf{A}_a \\ \mathbf{A}_b \end{Bmatrix} \tag{24}$$

where

$$\mathbf{k}_{g1} = \begin{bmatrix} \mathbf{n}_{1,1} & \mathbf{n}_{1,3} & \cdots & \mathbf{n}_{1,2i-1} & \cdots & \mathbf{n}_{1,2n-1} \\ \mathbf{n}_{3,1} & \mathbf{n}_{3,3} & \cdots & \mathbf{n}_{3,2i-1} & \cdots & \mathbf{n}_{3,2n-1} \\ \vdots & \vdots & \ddots & \vdots & \iddots & \vdots \\ \mathbf{n}_{2j-1,1} & \mathbf{n}_{2j-1,3} & \cdots & \mathbf{n}_{2j-1,2i-1} & \cdots & \mathbf{n}_{2j-1,2n-1} \\ \vdots & \vdots & \iddots & \vdots & \ddots & \vdots \\ \mathbf{n}_{2n-1,1} & \mathbf{n}_{2n-1,3} & \cdots & \mathbf{n}_{2n-1,2i-1} & \cdots & \mathbf{n}_{2n-1,2n-1} \end{bmatrix}, \mathbf{k}_{g2} = \begin{bmatrix} \mathbf{n}_{2,2} & \mathbf{n}_{2,4} & \cdots & \mathbf{n}_{2,2i} & \cdots & \mathbf{n}_{2,2n} \\ \mathbf{n}_{4,2} & \mathbf{n}_{4,4} & \cdots & \mathbf{n}_{4,2i} & \cdots & \mathbf{n}_{4,2n} \\ \vdots & \vdots & \ddots & \vdots & \iddots & \vdots \\ \mathbf{n}_{2j,2} & \mathbf{n}_{2j,4} & \cdots & \mathbf{n}_{2j,2i} & \cdots & \mathbf{n}_{2j,2n} \\ \vdots & \vdots & \iddots & \vdots & \ddots & \vdots \\ \mathbf{n}_{2n,2} & \mathbf{n}_{2n,4} & \cdots & \mathbf{n}_{2n,2i} & \cdots & \mathbf{n}_{2n,2n} \end{bmatrix}$$

$$\mathbf{K}_{g12} = \begin{bmatrix} \mathbf{n}_{1,2} & \mathbf{n}_{1,4} & \cdots & \mathbf{n}_{1,2i} & \cdots & \mathbf{n}_{1,2n} \\ \mathbf{n}_{3,2} & \mathbf{n}_{3,4} & \cdots & \mathbf{n}_{3,2i} & \cdots & \mathbf{n}_{3,2n} \\ \vdots & \vdots & \ddots & \vdots & \iddots & \vdots \\ \mathbf{n}_{2j-1,2} & \mathbf{n}_{2j-1,4} & \cdots & \mathbf{n}_{2j-1,2i} & \cdots & \mathbf{n}_{2j-1,2n} \\ \vdots & \vdots & \iddots & \vdots & \ddots & \vdots \\ \mathbf{n}_{2n-1,2} & \mathbf{n}_{2n-1.4} & \cdots & \mathbf{n}_{2n-1,2i} & \cdots & \mathbf{n}_{2n-1,2n} \end{bmatrix}, \quad \mathbf{n}_{j,i} = \left[\begin{array}{c|c} 0 & m_{5,i,j} \\ \hline m_{6,i,j} & 0 \end{array}\right] + b\left[\begin{array}{c|c} 0 & 0 \\ \hline 0 & m_{7,i,j} \end{array}\right]$$

(25)a-d

$$\begin{aligned} m_{5,i,j} &= -\frac{(j\pi)^2}{L}\beta(j,i,k_{max}) + (-1)^n\left(\frac{1}{L}\right)\left[(2n+1)\pi\right]^2 \sin\frac{j\pi}{2}\beta(2n+1,i,k_{max}) \\ m_{6,i,j} &= -\frac{(i\pi)^2}{L}\beta(i,j,k_{max}) + (-1)^n\left(\frac{1}{L}\right)\left[(2n+1)\pi\right]^2 \sin\frac{i\pi}{2}\beta(2n+1,j,k_{max}) \\ m_{7,i,j} &= (-1)^n\left(\frac{1}{L}\right)\left[(2n+1)\pi\right]^2 \beta(2n+1,j,k_{max})\sin\frac{i\pi}{2} \\ &\quad +(-1)^n\left(\frac{1}{L}\right)\left[(2n+1)\pi\right]^2 \beta(2n+1,i,k_{max})\sin\frac{j\pi}{2} \end{aligned} \tag{26}$$

$$\beta(i,j,k_{max})=\frac{1}{L}\int_0^L\sum_{k=1,2}^{kmax} m_k \sin\frac{i\pi z}{L}\sin\frac{j\pi z}{L}\sin\frac{k\pi z}{L}dz \tag{27}$$

Special considerations for symmetric loading

For loading symmetric with respect to $z = L/2$, bending moments are symmetric and Eq. (9) yields

$$M(z)=\sum_{k=1,3,5}^{kmax} m_k \sin\frac{k\pi z}{L} \tag{28}$$

where k takes only the values 1,3,5… Thus, when one of i, j is odd and the other is even, matrix $\mathbf{n}_{j,i}$ as defined in Eq. (25) can be shown to vanish. This is the case since function $\sin(i\pi z/L)\sin(j\pi z/L)$ is anti-symmetric with respect to $z = L/2$ and $\sum_{k=1,2}^{k_{max}} m_k \sin(i\pi z/L)\sin(j\pi z/L)\sin(k\pi z/L)$ in Eq. (27) is also anti-symmetric and

$$\beta(i,j,k_{max})=\frac{1}{L}\int_0^L\sum_{k=1,2}^{k_{max}} m_k \sin\frac{i\pi z}{L}\sin\frac{j\pi z}{L}\sin\frac{k\pi z}{L}dz=0 \tag{29}$$

Also, for the case where one of i, j is odd and the other is even, one can show that

$$\sin\frac{j\pi}{2}\beta(2n+1,i,k_{max})=\sin\frac{i\pi}{2}\beta(2n+1,j,k_{max})=0 \tag{30}$$

From Eq. (29) and (30) by substituting into Eq.(26), one has $\mathbf{n}_{j,i}=\mathbf{0}$ when one of i, j is odd and the other is even and thus $\mathbf{k}_{g12}=\mathbf{0}$, and Eq. (24) takes the form

$$V_1=\frac{\lambda}{2}\left\langle \mathbf{A}_a{}^T \quad \mathbf{A}_b{}^T \right\rangle \begin{bmatrix} \mathbf{k}_{g1} & \mathbf{0} \\ \mathbf{0} & \mathbf{k}_{g2} \end{bmatrix} \begin{Bmatrix} \mathbf{A}_a \\ \mathbf{A}_b \end{Bmatrix} \tag{31}$$

Destabilizing term due to load height effect

Case1- Mid-span load offset from section mid-height

A mid-span point load λQ can be mathematically expressed as $\lambda q(z) = \lambda Q\delta(z - L/2)$ where δ is the Dirac Delta function. If the load is acting at a distance a above the section mid-height, the load potential energy gain V_2 as determined from in Eq. (2)b takes the form

$$V_2 = -\frac{\lambda}{2}\int_0^L Q\delta\left(z-\frac{L}{2}\right)a\theta(z)^2\,dz = -\frac{\lambda}{2}Qa\theta\left(\frac{L}{2}\right)^2 = -\frac{\lambda}{2}Qa\sum_{i=1,2}^{2n}\sum_{j=1,2}^{2n}B_iB_j\sin\left(\frac{i\pi}{2}\right)\sin\left(\frac{j\pi}{2}\right) \quad (32)$$

In a matrix form, V_2 can be expressed as

$$V_2 = \frac{\lambda}{2}\left\langle \mathbf{A}_a{}^{\mathrm{T}} \quad \mathbf{A}_b{}^{\mathrm{T}} \right\rangle \begin{bmatrix} \mathbf{k}_{g3} & \mathbf{k}_{g34} \\ \mathbf{k}_{g34}^{\mathrm{T}} & \mathbf{k}_{g4} \end{bmatrix} \begin{Bmatrix} \mathbf{A}_a \\ \mathbf{A}_b \end{Bmatrix} \quad (33)$$

where

$$\mathbf{k}_{g3} = Qa\begin{bmatrix} \mathbf{r}_{1,1} & \mathbf{r}_{1,3} & \cdots & \mathbf{r}_{1,2i-1} & \cdots & \mathbf{r}_{1,2n-1} \\ \mathbf{r}_{3,1} & \mathbf{r}_{3,3} & \cdots & \mathbf{r}_{3,2i-1} & \cdots & \mathbf{r}_{3,2n-1} \\ \vdots & \vdots & \ddots & \vdots & \iddots & \vdots \\ \mathbf{r}_{2j-1,1} & \mathbf{r}_{2j-1,3} & \cdots & \mathbf{r}_{2j-1,2i-1} & \cdots & \mathbf{r}_{2j-1,2n-1} \\ \vdots & \vdots & \iddots & \vdots & \ddots & \vdots \\ \mathbf{r}_{2n-1,1} & \mathbf{r}_{2n-1,3} & \cdots & \mathbf{r}_{2n-1,2i-1} & \cdots & \mathbf{r}_{2n-1,2n-1} \end{bmatrix}, \mathbf{k}_{g4} = Qa\begin{bmatrix} \mathbf{r}_{2,2} & \mathbf{r}_{2,4} & \cdots & \mathbf{r}_{2,2i} & \cdots & \mathbf{r}_{2,2n} \\ \mathbf{r}_{4,2} & \mathbf{r}_{4,4} & \cdots & \mathbf{r}_{4,2i} & \cdots & \mathbf{r}_{4,2n} \\ \vdots & \vdots & \ddots & \vdots & \iddots & \vdots \\ \mathbf{r}_{2j,2} & \mathbf{r}_{2j,4} & \cdots & \mathbf{r}_{2j,2i} & \cdots & \mathbf{r}_{2j,2n} \\ \vdots & \vdots & \iddots & \vdots & \ddots & \vdots \\ \mathbf{r}_{2n,2} & \mathbf{r}_{2n,4} & \cdots & \mathbf{r}_{2n,2i} & \cdots & \mathbf{r}_{2n,2n} \end{bmatrix}$$

$$\mathbf{k}_{g34} = Qa\begin{bmatrix} \mathbf{r}_{1,2} & \mathbf{r}_{1,4} & \cdots & \mathbf{r}_{1,2i} & \cdots & \mathbf{r}_{1,2n} \\ \mathbf{r}_{3,2} & \mathbf{r}_{3,4} & \cdots & \mathbf{r}_{3,2i} & \cdots & \mathbf{r}_{3,2n} \\ \vdots & \vdots & \ddots & \vdots & \iddots & \vdots \\ \mathbf{r}_{2j-1,2} & \mathbf{r}_{2j-1,4} & \cdots & \mathbf{r}_{2j-1,2i} & \cdots & \mathbf{r}_{2j-1,2n} \\ \vdots & \vdots & \iddots & \vdots & \ddots & \vdots \\ \mathbf{r}_{2n-1,2} & \mathbf{r}_{2n-1.4} & \cdots & \mathbf{r}_{2n-1,2i} & \cdots & \mathbf{r}_{2n-1,2n} \end{bmatrix}, \quad \mathbf{r}_{j,i} = \left[\begin{array}{c|c} 0 & 0 \\ \hline 0 & \sin\frac{i\pi}{2}\sin\frac{j\pi}{2} \end{array}\right] \quad (34)$$

when either of i , j are even and the other is odd, the expression $\sin(i\pi/2)\sin(j\pi/2)$ vanishes. In this case, matrix $\mathbf{k}_{g34}$ vanishes and

$$V_2 = \frac{\lambda}{2}\left\langle \mathbf{A}_a{}^T \quad \mathbf{A}_b{}^T \right\rangle \begin{bmatrix} \mathbf{k}_{g3} & \mathbf{0} \\ \mathbf{0} & \mathbf{k}_{g4} \end{bmatrix}_{(1)} \begin{Bmatrix} \mathbf{A}_a \\ \mathbf{A}_b \end{Bmatrix} \tag{35}$$

Case2- Uniformly Distributed load offset from section mid-height

For the case of uniformly distributed load applied at height a above the section mid-height, the load potential gain can be expressed as

$$\begin{aligned} V_2 &= -\frac{\lambda}{2}\int_0^L qa\theta(z)^2\,dz = -\frac{\lambda}{2}qa\int_0^L \sum_{i=1,2}^{2n}\sum_{j=1,2}^{2n} B_i B_j \sin\left(\frac{i\pi z}{L}\right)\sin\left(\frac{j\pi z}{L}\right)dz \\ &= \frac{\lambda}{2}\left\langle \mathbf{A}_a{}^T \quad \mathbf{A}_b{}^T \right\rangle \begin{bmatrix} \mathbf{k}_{g3} & \mathbf{0} \\ \mathbf{0} & \mathbf{k}_{g4} \end{bmatrix}_{(2)} \begin{Bmatrix} \mathbf{A}_a \\ \mathbf{A}_b \end{Bmatrix} \end{aligned} \tag{36}$$

where

$$\mathbf{k}_{g3} = \mathbf{k}_{g4} = -\frac{1}{2}qLa\mathbf{Diag}(0,1,0,1...0,1) \tag{37}$$

Appendix B: Elastic and Geometric Matrices needed to determine critical bracing height.

As given by Eq. (15), the elastic stiffness matrix $\mathbf{k}_1$ can be re-written as the sum of three matrices

$$\mathbf{k}_1 = \bar{\mathbf{k}}_1 + b_{cr}\bar{\bar{\mathbf{k}}}_1 + b_{cr}^2\bar{\bar{\bar{\mathbf{k}}}}_1$$

where

$$\bar{\bar{\mathbf{k}}}_1 = \begin{bmatrix} \mathbf{m}''_{1,1} & \mathbf{m}''_{1,3} & \cdots & \mathbf{m}''_{1,2i-1} & \cdots & \mathbf{m}''_{1,2n-1} \\ \mathbf{m}''_{3,1} & \mathbf{m}''_{3,3} & \cdots & \mathbf{m}''_{3,2i-1} & \cdots & \mathbf{m}''_{3,2n-1} \\ \vdots & \vdots & \ddots & \vdots & \iddots & \vdots \\ \mathbf{m}''_{2j-1,1} & \mathbf{m}''_{2j-1,3} & \cdots & \mathbf{m}''_{2j-1,2i-1} & \cdots & \mathbf{m}''_{2j-1,2n-1} \\ \vdots & \vdots & \iddots & \vdots & \ddots & \vdots \\ \mathbf{m}''_{2n-1,1} & \mathbf{m}''_{2n-1,3} & \cdots & \mathbf{m}''_{2n-1,2i-1} & \cdots & \mathbf{m}''_{2n-1,2n-1} \end{bmatrix}, \bar{\bar{\mathbf{m}}}_{j,i} = \left[\begin{array}{c|c} 0 & m_2 \\ \hline m_2 & 0 \end{array}\right]$$

$$\bar{\bar{\bar{\mathbf{k}}}}_1 = \begin{bmatrix} \mathbf{m}'''_{1,1} & \mathbf{m}'''_{1,3} & \cdots & \mathbf{m}'''_{1,2i-1} & \cdots & \mathbf{m}'''_{1,2n-1} \\ \mathbf{m}'''_{3,1} & \mathbf{m}'''_{3,3} & \cdots & \mathbf{m}'''_{3,2i-1} & \cdots & \mathbf{m}'''_{3,2n-1} \\ \vdots & \vdots & \ddots & \vdots & \iddots & \vdots \\ \mathbf{m}'''_{2j-1,1} & \mathbf{m}'''_{2j-1,3} & \cdots & \mathbf{m}'''_{2j-1,2i-1} & \cdots & \mathbf{m}'''_{2j-1,2n-1} \\ \vdots & \vdots & \iddots & \vdots & \ddots & \vdots \\ \mathbf{m}'''_{2n-1,1} & \mathbf{m}'''_{2n-1,3} & \cdots & \mathbf{m}'''_{2n-1,2i-1} & \cdots & \mathbf{m}'''_{2n-1,2n-1} \end{bmatrix}, \bar{\bar{\bar{\mathbf{m}}}}_{j,i} = \left[\begin{array}{c|c} 0 & 0 \\ \hline 0 & m_4 \end{array}\right],$$

Also, as given by Eq. (16), the geometric stiffness matrix $\mathbf{k}_{g1}$ can be expressed by

$$\mathbf{k}_{g1} = \bar{\mathbf{k}}_{g1} + b_{cr}\bar{\bar{\mathbf{k}}}_{g1}$$

$$\bar{\mathbf{k}}_{g11} = \begin{bmatrix} \mathbf{n}'_{1,1} & \mathbf{n}'_{1,3} & \cdots & \mathbf{n}'_{1,2i-1} & \cdots & \mathbf{n}'_{1,2n-1} \\ \mathbf{n}'_{3,1} & \mathbf{n}'_{3,3} & \cdots & \mathbf{n}'_{3,2i-1} & \cdots & \mathbf{n}'_{3,2n-1} \\ \vdots & \vdots & \ddots & \vdots & \iddots & \vdots \\ \mathbf{n}'_{2j-1,1} & \mathbf{n}'_{2j-1,3} & \cdots & \mathbf{n}'_{2j-1,2i-1} & \cdots & \mathbf{n}'_{2j-1,2n-1} \\ \vdots & \vdots & \iddots & \vdots & \ddots & \vdots \\ \mathbf{n}'_{2n-1,1} & \mathbf{n}'_{2n-1,3} & \cdots & \mathbf{n}'_{2n-1,2i-1} & \cdots & \mathbf{n}'_{2n-1,2n-1} \end{bmatrix}, \bar{\mathbf{n}}_{j,i} = \left[\begin{array}{c|c} 0 & m_5 \\ \hline m_6 & 0 \end{array}\right]$$

558 $$\overline{\overline{\mathbf{k}}}_{g12} = \begin{bmatrix} \mathbf{n}''_{1,1} & \mathbf{n}''_{1,3} & \cdots & \mathbf{n}''_{1,2i-1} & \cdots & \mathbf{n}''_{1,2n-1} \\ \mathbf{n}''_{3,1} & \mathbf{n}''_{3,3} & \cdots & \mathbf{n}''_{3,2i-1} & \cdots & \mathbf{n}''_{3,2n-1} \\ \vdots & \vdots & \ddots & \vdots & \iddots & \vdots \\ \mathbf{n}''_{2j-1,1} & \mathbf{n}''_{2j-1,3} & \cdots & \mathbf{n}''_{2j-1,2i-1} & \cdots & \mathbf{n}''_{2j-1,2n-1} \\ \vdots & \vdots & \iddots & \vdots & \ddots & \vdots \\ \mathbf{n}''_{2n-1,1} & \mathbf{n}''_{2n-1,3} & \cdots & \mathbf{n}''_{2n-1,2i-1} & \cdots & \mathbf{n}''_{2n-1,2n-1} \end{bmatrix}, \overline{\overline{\mathbf{n}}}_{j,i} = \left[\begin{array}{c|c} 0 & 0 \\ \hline 0 & m_7 \end{array}\right]$$

559 **Acknowledgments**

560 The authors gratefully acknowledge funding from the Natural Sciences and Engineering Research
561 Council (NSERC) of Canada to the second and third authors.

562 **References**

563 [1] Austin, W.J., Yegian, S. Tung, T. P. (1955). “Lateral buckling of elastically end-restrained I-
564 beams.” *T. Am. Soc. Civ. Eng.*, 122(1), 374-388

565 [2] American Forest and Paper Association (AFPA). (2003). “Technical Report 14: Designing for
566 lateral torsional stability in wood members.” Washington, D.C., U.S.

567 [3] American Institution of Steel Construction (AISC). (2010). “Specification for structure steel
568 buildings.” ANSI/AISC 2010a. Chicago, U.S.

569 [4] American Institution of Steel Construction (AISC). (2010). “Commentary on the specification
570 for structure steel buildings.” ANSI/AISC 2010b. Chicago, U.S.

571 [5] Andrade, A., and Camotim, D. (2005). “Lateral-torsional buckling of singly symmetric tapered
572 beams: theory and applications.” *J. Eng. Mech.*, 131(6), 586-597

573 [6] Andrade, A., Camotim, D. Dinis, P.B. (2007). “Lateral-torsional buckling of singly symmetric
574 web-tapered thin-walled I-beams: 1D model vs. shell FEA.” *Comput. Struct.*, 85(17-18), 1343-
575 1359

576

577 [7] Canadian Standards Association (CSA). (2014). "Design of steel structures." S16-14.
578 Mississauga, Ontario, Canada.
579 [8] Canadian Standards Association (CSA) (2014), "Engineering Design in Wood", O86-14
580 Mississauga, Ontario, Canada
581 [9] Du, Y. Mohareb, M. and Doudak, G. (2016a), Nonsway Model for Lateral Torsional Buckling of
582 Wooden Beams under Wind Uplift, Journal of Engineering Mechanics, ASCE, ISSN 0733-9399
583 [10] Du, Y, Mohareb M., Doudak D (2016b) Lateral Torsional Buckling of Twin-beam deck assemblies
584 under wind uplift–sway versus non-sway models, World conference in timber engineering, Vienna Austria,
585 Aug. 22-25
586 [11] European Committee for Standardization (EC). (2005). "Design of steel structures part 1.1:
587 general rules and rules for buildings." EN 1993-1-1:2005. Brussels, Belgium.
588 [12] Erkmen, R.E. and Mohareb, M. (2008). "Buckling analysis of thin-walled open members-A
589 finite element formulation." *Thin. Wall. Struct.,* 46(6), 618-636
590 [13] Flint, A.R. (1951), "The influence of restraints on the stability of beams." *Struct. Eng.*, 29(9),
591 235-246
592 [14] Hooley, R. F., and Borg Madsen, (1964), "Lateral stability of glued laminated beams",
593 *Journal of the Structural Division*, 90(3), 201-218.
594 [15] Helwig, T., Frank, K., and Yura, J. (1997). "Lateral-torsional buckling of singly symmetric I-
595 beams." *J. Struct. Eng.,* 123(9), 1172-1179
596 [16] Ings, N.L. and Trahair, N.S. (1987). "Beam and column buckling under directed loading." *J.*
597 *Eng. Mech.*, 113(6), 1251-1263
598 [17] Jingping, L., Zaitian, G. Chen, S. (1988). "Buckling of transversely loaded I-Beam columns."
599 *J. Struct. Eng.*, 114(9), 2109-2118

600 [18] Kerensky, O.A., Flint, A.R., Brown, W.C. (1956). “The basis for design of beams and plate
601 girders in the revised British Standard 153.” *P. I. Civil. Eng.*, 5(3), 396–461
602 [19] Kitipomchai, S., Dux, P.F., Richter, N.J. (1984). “Buckling and bracing of cantilevers.” *J.*
603 *Struct. Eng.*, 110(9), 2250-2262
604 [20] Lay, M.G., Galambos, T.V., Schmidt, L.C. (1963). “Lateral bracing force of steel I beams.”
605 *J. Eng. Mech. Div.*, 89(EM3), 217-224
606 [21] Lamb, A.W., and Eamon, C.D. (2015). “Load height and moment factors for doubly
607 symmetric wide flange beams.” *J. Struct. Eng.*, 10.1061/(ASCE)ST.1943-541X.0001332,
608 04015069
609 [22] Mutton, B.R., and Trahair, N.S. (1973). “Stiffness requirement for lateral bracing.” *J. Struct.*
610 *Eng. Div.*, 99(10), 2167-2182
611 [23] Mohri, F., and Potier-Ferry, M. (2006). “Effects of load height application and pre-buckling
612 deflection on lateral buckling of thin-walled beams.” *Steel. Compos. Struct.*, 6(5), 1-15
613 [24] Mohebkhah, A. (2010). “Lateral buckling resistance of inelastic I-beams under off-shear
614 center loading.” *Thin. Wall. Struct.*, 49(3), 431-436
615 [25] McCann, F., Wadee, M.A., Gardner, L. (2013). “Lateral stability of imperfect discretely
616 braced steel beams.” *J. Eng. Mech.*, 139(10), 1341-1349
617 [26] Morkhade, S.G., and Gupta, L.M. (2013). “Effect of load height on buckling resistance of
618 steel beams.” *Procedia. Eng.*, 51, 151-158
619 [27] Nethercot, D.A., and Rockey, K.C. (1971). “A unified approach to the elastic lateral buckling
620 of beams.” *Struct. Eng.*, 49(7), 321-330
621 [28] Nethercot, D.A., and Rockey, K.C. (1972). “The lateral buckling of beams having discrete
622 intermediate restraints.” *Struct. Eng.*, 50(10), 391-403

623 [29] NDS (2015), National Design Specification for Wood Construction, American Wood council,
624 Leesburg, Virginia, USA
625 [30] Prescott, J., and Carrington, H. (1920). "The Buckling of deep beams." *Phil. Mag.*, 39(230),
626 194-233
627 [31] Pettersson, O. (1952). "Combined bending and torsion of I-beams of monosymmetrical cross
628 section." Bulletin No.10, *Division of Building Statics and Structural Engineering*, Royal Institute
629 of Technology, Stockholm, Sweden
630 [32] Pi, Y.L., Traihair, N.S., Rajasekaran, S. (1992). "Energy equation for beam lateral buckling."
631 *J. Struct. Eng.*, 118(6), 1462-1479
632 [33] Park, J.S., Stalling, M.J., Kang, Y.J. (2004). "Lateral-torsional buckling of prismatic beams
633 with continuous top flange bracing." *J. Constr. Steel. Res.*, 60(2), 147–160
634 [34] Pai, PF. Highly flexible structures: modeling, computation, and experimentation, AIAA
635 Educational Series; 2007.
636 [35] Sahraei, A., Wu, L., Mohareb, M. (2015). "Finite element formulation for lateral torsional
637 buckling analysis of shear deformable mono-symmetric thin-walled members." *Thin. Wall. Struct.*,
638 doi:10.1016/j.tws.2014.11.023
639 [36] Samanta, A., and Kumar, A. (2006). "Distortional buckling in monosymmetric I-beams." *Thin.*
640 *Wall. Struct.,* 44(1), 51-56
641 [37] Samanta, A., Kumar, A. (2008). "Distortional buckling in braced-cantilever I-beams." *Thin.*
642 *Wall. Struct.*, 46(6), 637-645
643 [38] Schmidt, L.C., (1965). "Restraints against elastic lateral buckling." *J. Eng. Mech. Div.*,
644 91(EM6), 1-10

645 [39] Schrader, R.K. (1941). “Discussion of paper by G. Winter.” *T. Am. Soc. Civ. Eng.*, 108(1),
646 260-268
647 [40] Standards Australia (SA). (1998). “Steel structures. Australian standard AS 4100-1998.”
648 Homebush, Australia.
649 [41] Timoshenko, S. (1936). *Theory of elastic stability*, McGraw-Hill Book Company, Inc., New
650 York
651 [42] Tong, G.S., and Chen, S.F. (1988). “Buckling of laterally torsionally braced beams.” *J. Constr.*
652 *Steel. Res.*, 11(1), 41-55
653 [43] Trahair, N.S. (1993). *Flexural-Torsional Buckling of Structures*. E & FN Spon, London.
654 [44] Trahair, N.S. (2013). “Bending and buckling of tapered steel beam structures.” *Eng. Struct.*,
655 59, 229-237
656 [45] Wang, C.M., Kitrporncha, S. Thevendran, V. (1987). “Buckling of braced monosymmetric
657 cantilevers.” *Int. J. Mech. Sci.*, 29(5), 321-337
658 [46] White, D.W., and Kim, Y.D. (2008). “Unified Flexural Resistance Equations for Stability
659 Design of Steel I-Section Members: Moment Gradient Tests.” *J. Struct. Eng.,* 134(9), 1450-1470
660 [47] Winter, G. (1941). “Lateral stability of unsymmetrical I-beams and trusses in bending.” *T.*
661 *Am. Soc. Civ. Eng.*, 108(1), 247-260
662 [48] Winter, G. (1960). “Lateral bracing of columns and beams.” *T. Am. Soc. Civ. Eng.,* 125 (1),
663 807-826
664 [49] Wong, E., Driver, R.G., Heal, T.W. (2015). “Simplified approach to estimating the elastic
665 lateral–torsional buckling capacity of steel beams with top-flange loading.” *Can. J. Civil. Eng.*,
666 42(2), 130-138

667 [50] Wong-Chung, A.D., and Kitipomchai, S. (1987). “Partially braced inelastic beam buckling
668 experiments.” *J. Constr. Steel. Res.,* 7(3), 189-211
669 [51] Wu, L., and Mohareb, M. (2010). “Buckling formulation for shear deformable thin-walled
670 members-II. Finite element formulation.” *Thin. Wall. Struct.,* 49(1), 208-222
671 [52] Xiao, Q, (2014), Lateral torsional buckling of wood beams, MASc thesis, Department of
672 Civil Engineering, University of Ottawa.
673 [53] Xiao, Q, Doudak, G, and Mohareb, M (2014), lateral torsional buckling of wood beams: FEA-
674 modelling and sensitivity analysis, World Conference in Timber Engineering, Quebec City,
675 Quebec, Canada, August 10-14
676 [54] Yura, J.A. (2001). “Fundamental of Beam Bracing.” *Eng. J.*, 38(1), 11-26
677 [55] Yura, J.A., Helwig, T.A., Zhou, C. (2008). “Global lateral buckling of I-shaped girder system.”
678 *J. Struct. Eng.*, 134(9), 1487-1494

679 **Table 1 Assessing accuracy of bracing heights predictions**

	a/h	bcr/h-based on simplified expression	bcr/h-based on ABAQUS	Difference
Point load	-0.25	-0.458	-0.495	3.72%
	0.00	-0.286	-0.289	0.26%
	0.25	-0.115	-0.123	0.80%
	0.50	0.057	0.107	4.96%
Uniformly distributed load	-0.25	-0.410	-0.433	2.25%
	0.00	-0.346	-0.330	1.62%
	0.25	-0.263	-0.242	2.08%
	0.50	-0.158	-0.138	2.00%

680

681

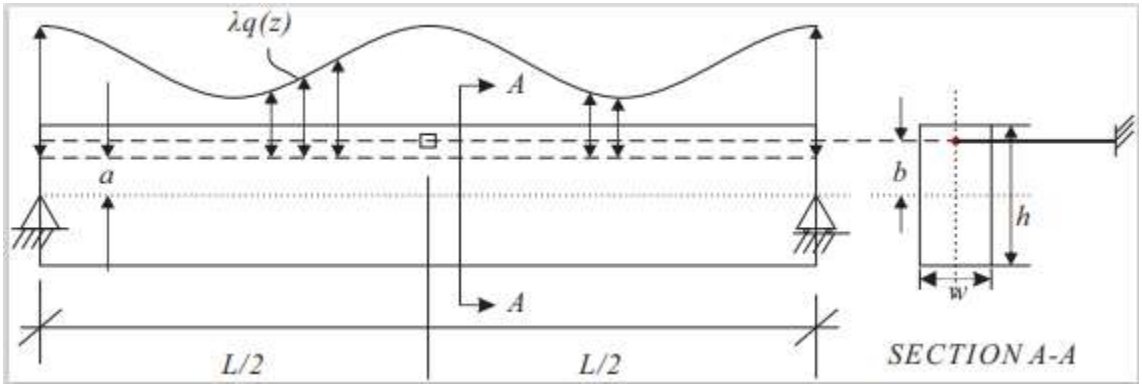

682

683 **Fig.1** Load height and brace effect

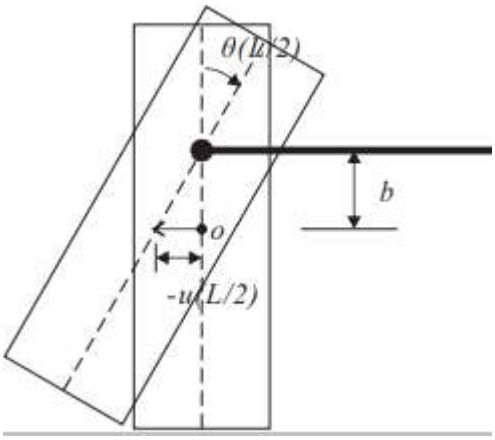

684

685 **Fig.2** Beam cross section at mid-span

686

687

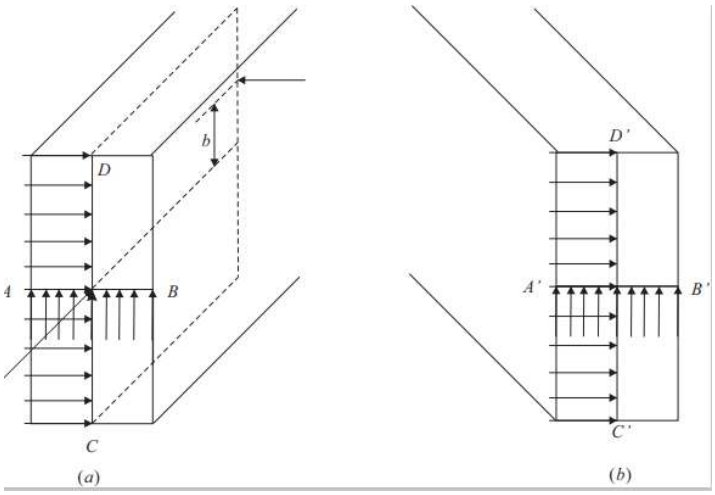

688

689 **Fig. 3** Boundary conditions (all arrows denote restrained degree of freedoms) (a) left end (b) right end

690

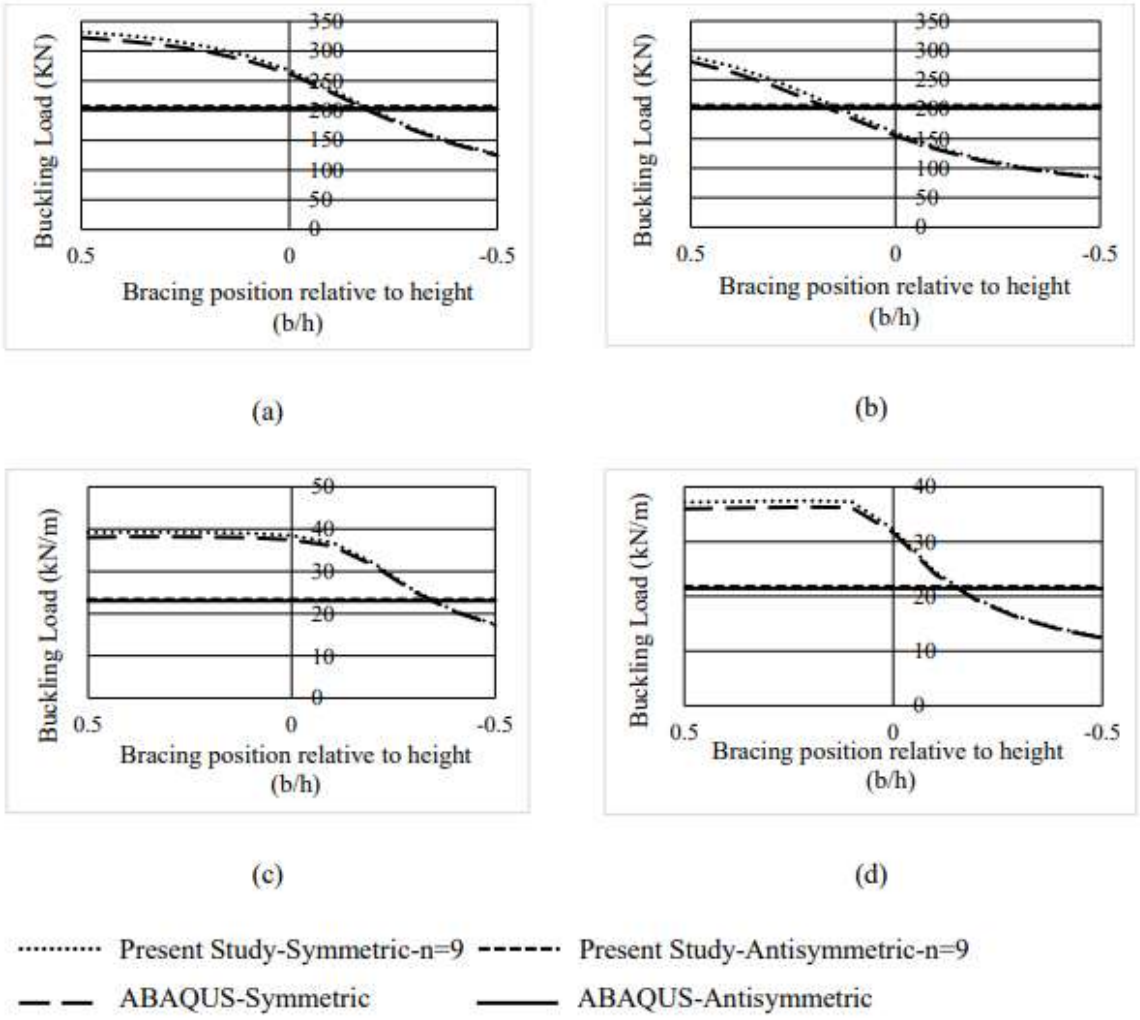

691

692 **Fig. 4** Buckling load comparison relative to different bracing height when load is (a) point load, mid-height a = 0
693 (b) point load, top face a = 0.5h (c) uniformly distributed load, mid-heighta = 0 (d) uniformly distributed load, top
694 face a = 0.5h

695

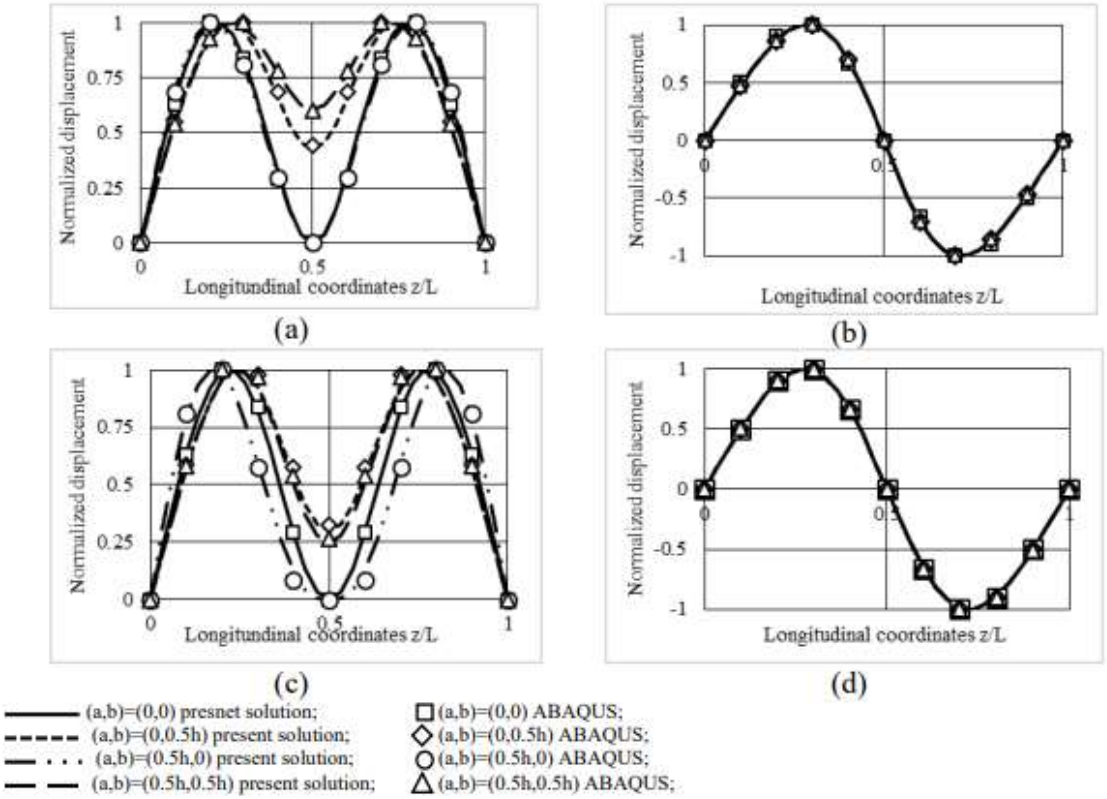

696

697 **Fig.5** Comparison of buckling mode shapes between present study and ABAQUS (a) point load-symmetric mode,
698 (b) point load-anti-symmetric mode, (c) uniformly distributed load-symmetric mode, and (d) uniformly distributed
699 load-anti-symmetric mode

700

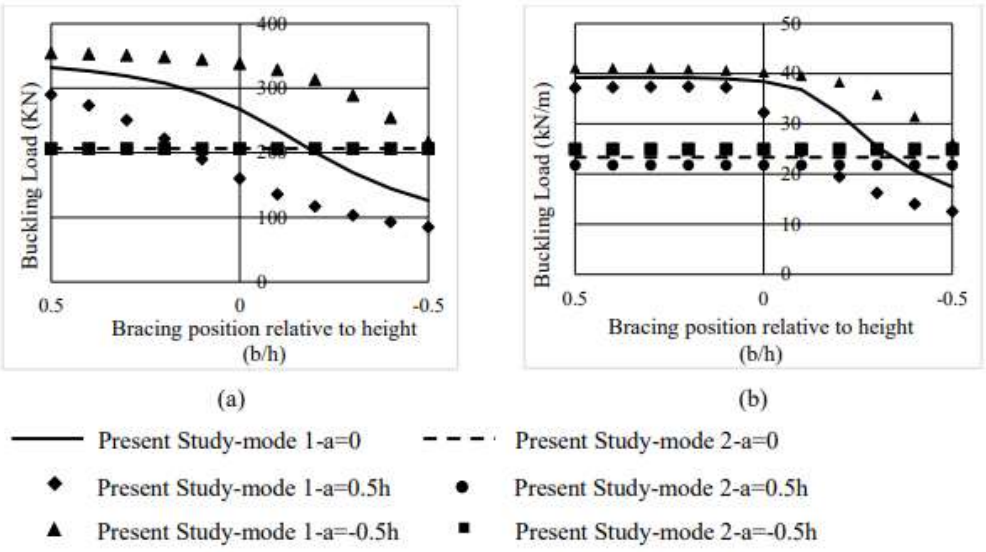

701

702 **Fig. 6** Effect of brace position under for different load heights (a) point load (b) uniformly distributed load